# Physical limitations on the scattering of electromagnetic vector spherical waves

Bernland, Anders; Gustafsson, Mats; Nordebo, Sven

2010

CODEN:LUTEDX/(TEAT-7194)/1-24/(2010)

Revision No. 1: August 2010

# Physical Limitations on the Scattering of Electromagnetic Vector Spherical Waves

**Anders Bernland, Mats Gustafsson, and Sven Nordebo**

Electromagnetic Theory
Department of Electrical and Information Technology
Lund University
Sweden

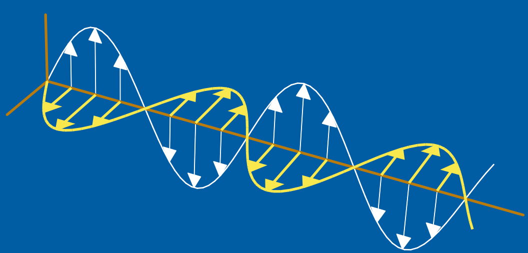

Anders Bernland and Mats Gustafsson
{Anders.Bernland,Mats.Gustafsson}@eit.lth.se

Department of Electrical and Information Technology
Electromagnetic Theory
Lund University
P.O. Box 118
SE-221 00 Lund
Sweden

Sven Nordebo
sven.nordebo@msi.vxu.se

School of Mathematics and Systems Engineering
Växjö University
SE-351 95 Växjö
Sweden

Department of Electrical and Information Technology
Electromagnetic Theory
Lund University
P.O. Box 118
SE-221 00 Lund
Sweden

Editor: Gerhard Kristensson

**Abstract**

Understanding the interaction between electromagnetic waves and matter is vital in applications ranging from classical optics to antenna theory. This paper derives physical limitations on the scattering of electromagnetic vector spherical waves. The assumptions made are that the heterogeneous scatterer is passive, and has constitutive relations which are on convolution form in the time domain and anisotropic in the static limit. The resulting bounds limit the reflection coefficient of the modes over a frequency interval, and can thus be interpreted as limitations on the absorption of power from a single mode. They can be used within a wide range of applications, and are particularly useful for electrically small scatterers. The derivation follows a general approach to derive sum rules and physical limitations on passive systems on convolution form. The time domain versions of the vector spherical waves are used to describe the passivity of the scatterer, and a set of integral identities for Herglotz functions are applied to derive sum rules from which the physical limitations follow.

# 1 Introduction

Understanding how electromagnetic fields interact with matter is vital in classical science, like optics and scattering theory, but also in modern applications like wireless communication, cloaking and metamaterials. When interacting with various objects, electromagnetic waves may be scattered and/or absorbed. If the objects are small compared to the wavelength, this interaction is limited. An early paper addressing these limits is Purcell's [19], discussing radiation emission and absorption by interstellar dust. Results similar to Purcell's can also be found in [3]. Limitations on antenna performance where introduced by Chu in [5]. Sohl et al. derives limitations on the extinction cross sections of arbitrary heterogeneous, anisotropic objects in [23], results that are directly applicable to antenna theory [8]. A summary of some important results on physical limitations on antennas can be found in Hansen's book [12]. More general dispersion relations for electromagnetic as well as quantum-mechanical scattering are discussed in *e.g.*, [13, 17] and references therein.

Electromagnetic fields can be decomposed into orthogonal vector spherical waves [11], also referred to as partial waves, (electric and magnetic) multipoles, or (TM and TE) modes. Such a decomposition is very beneficial in scattering theory. In wireless communication, these orthogonal modes are closely related to the orthogonal communication channels of multiple-input multiple-output (MIMO) systems [7].

The present paper seems to be the first to derive physical limitations on the scattering and absorption of electromagnetic vector spherical waves. To do so, a general approach to obtain sum rules and physical limitations for passive systems on convolution form put forth in [2] is used. At the core of this approach is a set of integral identities for Herglotz functions, a class of functions that is intimately linked to the transfer functions of passive systems.

The main results of this paper are physical limitations on the reflection coefficients of the modes for arbitrary heterogeneous, passive scatterers with constitutive relations on convolution form, and anisotropic in the static limit. The bounds state that the reflection coefficient cannot be arbitrarily small over a frequency interval of non-zero length; how small it can be depends upon the smallest sphere circumscribing the scatterer, its static material properties and the fractional bandwidth. An interpretation of the bounds on the reflection coefficients is as bounds on the maximum absorption of power from a single mode. The bounds are particularly useful for electrically small scatterers, and so they are well suited to analyse subwavelength particles designed to be resonant in one or more frequency bands, like antennas and metamaterials.

This paper is divided into sections as follows: First, in Section 2, the general approach to derive sum rules and physical limitations for passive systems presented in [2] is reviewed. In order to use this method and obtain the bounds in this paper, expressions for the vector spherical waves in both the time and frequency domains are needed. This is the topic of Section 3. In Section 4, the scattering matrix is introduced, and the physical limitations are derived. After this comes two examples in Section 5, one which discusses absorption of power in nanoshells, and another which considers limitations on antenna performance. Last come some concluding remarks in Section 6.

# 2 A general approach to obtain sum rules and physical limitations on passive systems

The derivation of the physical limitations on scattering of vector spherical waves in this paper follows a general approach to obtain sum rules and physical limitations for passive systems on convolution form presented in [2]. This section summarises this general approach in order to put the following sections in the right context. The general approach is described more thoroughly in [2], where all the necessary proofs can be found.

There are three major steps to obtain sum rules for a physical system: First, the transfer function of the system is related to a Herglotz function $h$. Secondly, the low-frequency asymptotic expansion of the transfer function is determined. This step commonly uses physical arguments, and is specific to each application. Then a set of integral identities for Herglotz functions, relating weighted integrals of $h$ to its low-frequency asymptotic expansion, is used. Essentially, this relates the dynamical behaviour of the physical system to its static properties. In the third step, physical limitations are derived by estimating the integral. Variational principles can sometimes be applied to the static parameters if they are unknown.

## 2.1 Herglotz functions and integral identities

Here the class of Herglotz functions is reviewed briefly, and the integral identities used to obtain sum rules for passive systems are presented. A Herglotz function $h$ is defined as a function holomorphic in $\mathbb{C}^+ = \{z, \operatorname{Im} z > 0\}$, satisfying $\operatorname{Im} h(z) \geq 0$ there. Furthermore, many Herglotz functions appearing in various applications are

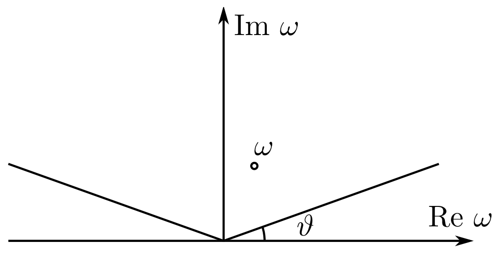


**Figure 1**: The cone $\{\omega : \vartheta \leq \arg\omega \leq \pi - \vartheta\}$ for some $\vartheta \in (0, \pi/2]$.

of the form $h(\omega) = \alpha + h_1(\omega)$, where $h_1$ exhibits the symmetry $h_1(\omega) = -h_1^*(-\omega^*)$ and $\alpha \in \mathbb{R}$ [2]. Such a function $h$ is called symmetric in this paper, and it satisfies the low-frequency expansion

$$h(\omega) = \alpha + \sum_{n=0}^{N} A_{2n-1}\omega^{2n-1} + \mathrm{o}(\omega^{2N-1}), \quad \text{as } \omega \hat{\to} 0, \tag{2.1}$$

for some integer $N \geq 0$. Here $A_{-1} \leq 0$ and all $A_n$ are real. The limit $\omega \hat{\to} 0$ is a short-hand notation for $|\omega| \to 0$ for $\omega$ in the cone $\vartheta \leq \arg\omega \leq \pi - \vartheta$ for any $\vartheta \in (0, \pi/2]$, see Figure 1. The asymptotic expansion (2.1) is clearly valid as $\omega \to 0$ for any argument in the case $h$ is holomorphic in a neighbourhood of the origin.

There is a set of integral identities for a symmetric Herglotz function $h$ [2]:

$$\lim_{\varepsilon\to 0^+} \lim_{\omega''\to 0^+} \frac{2}{\pi} \int_{\varepsilon}^{\infty} \frac{\operatorname{Im} h(\omega' + \mathrm{i}\omega'')}{\omega'^{2p}} \, \mathrm{d}\omega' = A_{2p-1} - \delta_{p,1}\beta, \quad p = 1, 2 \ldots, N. \tag{2.2}$$

Here $\delta_{p,q}$ denotes the Kronecker delta and $\beta = \lim_{\omega \hat{\to} \infty} h(\omega)/\omega \geq 0$, which always exists finitely. The Herglotz function $h$ is not necessarily holomorphic in a neighbourhood of the real line, but the distributional limit $\lim_{\omega''\to 0^+} h(\omega' + \mathrm{i}\omega'') \stackrel{\text{def}}{=} h(\omega')$ exists. The notation $\omega' = \operatorname{Re}\omega$ and $\omega'' = \operatorname{Im}\omega$ is used throughout this paper. The left-hand side of (2.2) is the integral of $\operatorname{Im} h(\omega')/\omega'^{2p}$ in the distributional sense, *i.e.*, contributions from possible singularities in the interval $(0, \infty)$ are included [2].

## 2.2 Sum rules for passive systems

Having introduced Herglotz functions, it remains to discuss the link between this class of functions and the transfer functions of passive systems on convolution form, *i.e.*, the first step of the general approach. The results presented here relies mainly on the work by Youla et. al. [26], Zemanian [27–29] and Wohlers and Beltrami [25]. See also the book [17] by Nussenzveig. How the integral identities (2.2) can be used to derive sum rules for such systems once the low-frequency asymptotic behaviour of the transfer function has been determined is also explained in this section.

Consider a general mathematical model of a physical system in the time domain, $u(t) = \mathcal{R}v(t)$, where $v$ and $u$ are the input and output signals, respectively, related to each other by the operator $\mathcal{R}$. The context of distributions is natural, since generalised functions such as the delta function should be allowed; hence, the domain $D(\mathcal{R})$ of the operator $\mathcal{R}$ is assumed to be some subset of the space of distributions $\mathcal{D}'$. The assumptions of linearity, continuity, and time-translational invariance imply that the operator is on convolution form [28], *i.e.*,

$$u(t) = \mathcal{R}v(t) = w * v(t). \tag{2.3}$$

Such a system is fully described by its impulse response $w$. Many physical systems obey causality, which intuitively means that the output cannot precede the input. For the mathematical model (2.3) it means that $\operatorname{supp} w \subseteq [0, \infty)$ [28].

Another crucial assumption is that of passivity; if the power of the input (output) signal at the time $t$ is $|v(t)|^2$ ($|u(t)|^2$), the power absorbed by the system is $|v(t)|^2 - |u(t)|^2$. In this paper, a system is defined to be passive if the energy expression

$$e(T) = \int_{-\infty}^{T} |v(t)|^2 - |u(t)|^2 \,\mathrm{d}t \tag{2.4}$$

is non-negative for all $T \in \mathbb{R}$ and $v \in \mathcal{D}$, where $\mathcal{D}$ denotes smooth functions of compact support [25, 29].[1] Only input signals $v \in \mathcal{D}$ are considered in order for the integral to be well-defined. However, this is often enough to ensure that the corresponding energy expressions are non-negative for other admissible input signals $v \in D(\mathcal{R})$.

One might expect that passive systems must be causal, and it turns out that this expectation is correct for operators on convolution form [26, 29]. Also, passivity implies that the impulse response is a distribution of slow growth [25, 29], $w \in \mathcal{S}'$ and hence Fourier transformable in the distributional sense. In this paper, the Fourier transform for all such distributions $f$ is defined through $\langle \mathcal{F}f, \varphi \rangle = \langle f, \mathcal{F}\varphi \rangle$ for all $\varphi \in \mathcal{S}$. Here $\mathcal{S}$ denotes the set of smooth functions of rapid descent, $\langle f, \varphi \rangle$ is the value in $\mathbb{C}$ that $f \in \mathcal{S}'$ assigns to $\varphi \in \mathcal{S}$ [28], and the Fourier transform of $\varphi$ is defined as $\mathcal{F}\varphi(\omega) = \int_{\mathbb{R}} \varphi(t) \mathrm{e}^{\mathrm{i}\omega t} \,\mathrm{d}t$. The frequency domain version of (2.3) is $\tilde{u}(\omega) = \tilde{w}(\omega)\tilde{v}(\omega)$, where the transfer function of the system is given by

$$\tilde{w}(\omega) = (\mathcal{F}w)(\omega),$$

and $\tilde{v} = \mathcal{F}v$ and $\tilde{u} = \mathcal{F}u$ are the input and output signals, respectively [2].

Passivity implies that the region of convergence for $\tilde{w}$ contains $\mathbb{C}^+$ and $\tilde{w}$ is holomorphic there. Furthermore, the transfer-function $\tilde{w}(\omega)$ is bounded in magnitude by one for $\omega \in \mathbb{C}^+$ [25, 29]. The transfer function $\tilde{w}$ is not necessarily holomorphic in a neighbourhood of the real axis, but $\tilde{w}(\omega') = \lim_{\omega'' \to 0} \tilde{w}(\omega' + \mathrm{i}\omega'')$ is well-defined for almost all $\omega' \in \mathbb{R}$ and bounded in magnitude by one [16].

One more assumption on the physical system is convenient (but not necessary): It is assumed that it maps real-valued input signals to real-valued output, which means that $w$ is real. This implies the symmetry

$$\tilde{w}(\omega) = \tilde{w}^*(-\omega^*), \quad \operatorname{Im} \omega > 0, \tag{2.5}$$

[1] This is not the only way to classify passive systems, see [2, 26, 28].

where the superscript $^*$ is used to denote the complex conjugate.

A Herglotz function can be constructed from $\tilde{w}$ in two ways, either with the inverse Cayley transform of $\pm\tilde{w}$, or by taking the complex logarithm of $\tilde{w}$ [2]. The latter way is chosen here. It requires that the zeros of $\tilde{w}$ are removed, which is done with a Blaschke-product. The Herglotz function is therefore

$$h(\omega) = -\mathrm{i}\log\left(\frac{\tilde{w}(\omega)}{B(\omega)}\right), \tag{2.6}$$

where

$$B(\omega) = \prod_{\omega_n} \frac{1-\omega/\omega_n}{1-\omega/\omega_n^*} \tag{2.7}$$

is a Blaschke product [16], repeating the possible zeros $\omega_n$ of $\tilde{w}$ in $\mathbb{C}^+$ according to their multiplicity. The logarithm is defined in [2]. The symmetry (2.5) implies that $h(\omega)$ is symmetric in the sense discussed in Section 2.1, with $\alpha = \arg\tilde{w}(\mathrm{i}\omega'')$.

The integral identities (2.2) applied to the function in (2.6) yield

$$\lim_{\varepsilon\to 0^+}\lim_{\omega''\to 0^+}\frac{2}{\pi}\int_\varepsilon^\infty \frac{1}{\omega'^{2p}}\ln\frac{1}{|\tilde{w}(\omega'+\mathrm{i}\omega'')|}\,\mathrm{d}\omega' = A_{2p-1} - \delta_{p,1}\beta, \quad p = 1,2\ldots,N, \tag{2.8}$$

where it has been used that $|B(\omega'+\mathrm{i}\omega'')| \to 1$ as $\omega'' \to 0$ for almost all $\omega' \in \mathbb{R}$ [16].[2] The low-frequency asymptotic expansion in (2.1) may be related to the behaviour of $\tilde{w}(\omega)$ as $\omega\hat{\to}0$, where as before $\omega\hat{\to}0$ is short-hand notation for $|\omega| \to 0$ for $\omega$ in the cone $\vartheta \leq \arg\omega \leq \pi - \vartheta$ for any $\vartheta \in (0, \pi/2]$. The cone assures that the low-frequency limit is only dependent on the behaviour of $w(t)$ for arbitrarily large times $t$ [2]. If, however, $\tilde{w}(\omega)$ is holomorphic in a neighbourhood of the origin, the low frequency limit is identical whatever the argument of $\omega$. The asymptotic behaviour of $\tilde{w}(\omega)$ as $\omega\hat{\to}0$ must be found by physical arguments specific to each application, and constitutes the second step of the general three-step approach [2]. In the third step, physical limitations may be derived by considering integrals over finite frequency intervals, since the integrand in (2.8) is non-negative. In some cases, variational principles are used to bound the expansion coefficients $A_p$ of $h$ when they are unknown.

# 3 Vector spherical waves in the time and frequency domains

Expansions of the electric and magnetic fields in vector spherical waves are widely employed in the frequency domain, see *e.g.*, [11]. Their counterparts in the time

[2]It might be that $\tilde{w}(\omega)$ has an accumulation point of zeros for one or more $\omega_j \in \mathbb{R}$, in which case $B(\omega_j + \mathrm{i}\omega'')$ does not tend to 1 as $\omega'' \to 0$. Then the Blaschke product must be included for the left-hand side to make sense, *i.e.*, (2.8) reads [2]:

$$\lim_{\varepsilon\to 0^+}\lim_{\omega''\to 0^+}\frac{2}{\pi}\int_\varepsilon^\infty \frac{1}{\omega'^{2p}}\ln\frac{|B(\omega'+\mathrm{i}\omega'')|}{|\tilde{w}(\omega'+\mathrm{i}\omega'')|}\,\mathrm{d}\omega' = A_{2p-1} - \delta_{p,1}\beta, \quad p = 1,2\ldots,N. \tag{2.9}$$

Equation (2.8) is understood to be replaced by (2.9) whenever necessary throughout this paper.

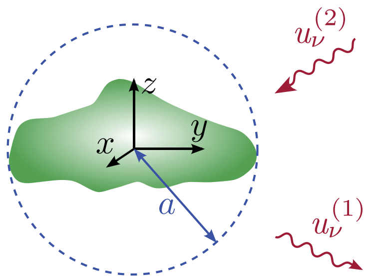


**Figure 2**: The scatterer is contained in a sphere of radius $a$ centered at the origin. Outside this sphere, the electric and magnetic fields are expanded in outgoing and incoming vector spherical waves, $\boldsymbol{u}_\nu^{(1)}$ and $\boldsymbol{u}_\nu^{(2)}$, with index $\nu$.

domain have been treated by Shlivinski and Heyman [20, 21]. Both the time and frequency domain vector spherical waves are considered in this section, since they are both required in Section 4 to derive physical limitations for passive scatterers according to the general approach described in Section 2; the time domain waves are necessary in order to rigorously describe passive scatterers and find their corresponding Herglotz functions, whereas the frequency domain counterparts are needed to derive the low-frequency behaviour of the scatterer and determine sum rules and physical limitations. A tilde ($\tilde{}$) is used in the remainder of this paper to denote functions in the frequency domain, and it is also convenient to employ the wavenumber $k = \omega/\mathrm{c}$, so that $\tilde{f}(k) = \mathcal{F}f(\omega)$. Here c is the speed of light in free space.

Consider an object in free space, and let $a$ be the radius of a sphere (centered at the origin) containing the object, see Figure 2. Outside this sphere, the electric field is expanded in outgoing and incoming vector spherical waves, denoted $\boldsymbol{u}_\nu^{(1)}$ and $\boldsymbol{u}_\nu^{(2)}$, respectively:

$$\widetilde{\boldsymbol{E}}(\boldsymbol{r}, k) = k\sqrt{\eta_0}\sum_\nu \mathrm{i}^{l+2-\tau}\tilde{b}_\nu^{(1)}(k)\boldsymbol{u}_\nu^{(1)}(k\boldsymbol{r}) + \mathrm{i}^{l+2-\tau}\tilde{b}_\nu^{(2)}(k)\boldsymbol{u}_\nu^{(2)}(k\boldsymbol{r}). \tag{3.1}$$

Here $\eta_0$ is the wave impedance in free space. The spatial coordinate is denoted $\boldsymbol{r}$, and in the rest of the paper the notation $r = |\boldsymbol{r}|$ and $\hat{\boldsymbol{r}} = \boldsymbol{r}/r$ is employed. For a definition of the vector spherical waves, see Appendix A.1. The multi-index $\nu = \{\tau, s, m, l\}$ is introduced to simplify the notation, and the factors $k\sqrt{\eta_0}\mathrm{i}^{l+2-\tau}$ are included for consistency with the time domain expansion described below. The corresponding magnetic field is

$$\widetilde{\boldsymbol{H}}(\boldsymbol{r}, k) = \frac{k}{\sqrt{\eta_0}}\sum_\nu \mathrm{i}^{l+1-\tau}\tilde{b}_\nu^{(1)}(k)\boldsymbol{u}_{\bar{\nu}}^{(1)}(k\boldsymbol{r}) + \mathrm{i}^{l+1-\tau}\tilde{b}_\nu^{(2)}(k)\boldsymbol{u}_{\bar{\nu}}^{(2)}(k\boldsymbol{r}), \tag{3.2}$$

where the dual multi-index $\bar{\nu} = \{\bar{\tau}, s, m, l\}$ with $\bar{\tau} = 3 - \tau$ has been introduced.

Outgoing vector spherical waves in the time domain are described thoroughly in [20, 21]. A short description, also covering incoming waves, is included here for clarity. Assuming that the fields vanish as $t \to -\infty$, the inverse Laplace transform may be applied to (3.1)–(3.2) with $k = \mathrm{i}s/\mathrm{c}$ and the integration curve over $s$ sufficiently far into the right half-plane. Using the explicit expressions (A.1) for the vector spherical waves yields the transverse electric field $\widetilde{\boldsymbol{E}}_{\mathrm{T}} = \widetilde{\boldsymbol{E}} - \hat{\boldsymbol{r}}(\hat{\boldsymbol{r}} \cdot \widetilde{\boldsymbol{E}})$:

$$\widetilde{\boldsymbol{E}}_{\mathrm{T}}(\boldsymbol{r}, k) = \frac{\sqrt{\eta_0}}{r} \sum_{\nu} \left[ \tilde{b}_{\nu}^{(1)}(k) \mathrm{e}^{-sr/\mathrm{c}} R_{\tau,l}^{(1)}(sr/\mathrm{c}) + \tilde{b}_{\nu}^{(2)}(k) \mathrm{e}^{sr/\mathrm{c}} R_{\tau,l}^{(2)}(sr/\mathrm{c}) \right] \boldsymbol{A}_{\nu}(\hat{\boldsymbol{r}}), \quad (3.3)$$

where

$$\begin{cases} R_{1,l}^{(1)}(s) = \sum_{n=0}^{l} D_{n,l} s^{-n} \\ R_{1,l}^{(2)}(s) = (-1)^{l-1} R_{1,l}^{(1)}(-s) \\ R_{2,l}^{(j)}(s) = R_{1,l-1}^{(j)}(s) + \dfrac{l}{s} R_{1,l}^{(j)}(s), \quad j = 1, 2, \end{cases}$$

and $D_{n,l} = (l+n)!/(2^n n!(l-n)!)$ according to (A.6). The vector spherical harmonics $\boldsymbol{A}_{\nu}$ are defined in Appendix A.1. Applying the inverse Laplace transform yields

$$\boldsymbol{E}_{\mathrm{T}}(\boldsymbol{r}, t) = \frac{\sqrt{\eta_0}}{r} \sum_{\nu} \left[ \mathcal{R}_{\tau,l}^{(1)} b_{\nu}^{(1)}(t - r/\mathrm{c}) + \mathcal{R}_{\tau,l}^{(2)} b_{\nu}^{(2)}(t + r/\mathrm{c}) \right] \boldsymbol{A}_{\nu}(\hat{\boldsymbol{r}}).$$

Here the operators $\mathcal{R}_{\tau,l}^{(j)} : \mathcal{D} \to \mathcal{D}$ in the time domain are defined by

$$\begin{cases} \mathcal{R}_{1,l}^{(j)} f(t) = (\pm 1)^{l-1} \sum_{n=0}^{l} D_{n,l} \left( \pm \dfrac{\mathrm{c}}{r} \, \mathrm{d}_t^{-1} \right)^n f(t) \\ \mathcal{R}_{2,l}^{(j)} f(t) = \mathcal{R}_{1,l-1}^{(j)} f(t) \pm l \dfrac{\mathrm{c}}{r} \, \mathrm{d}_t^{-1} \mathcal{R}_{1,l}^{(j)} f(t), \end{cases}$$

where the upper (lower) signs are for $j = 1$ ($j = 2$). The inverse to differentiation $\mathrm{d}_t^{-1}$ is chosen so that $\mathrm{d}_t^{-1} f(t)$ is the distributional primitive to $f$ that vanishes at $t = -\infty$, *i.e.*, $\mathrm{d}_t^{-1} f(t) = \int_{-\infty}^{t} f(t') \, \mathrm{d}t'$ for regular functions $f$. A similar representation is used for the magnetic field, giving

$$\boldsymbol{H}_{\mathrm{T}}(\boldsymbol{r}, t) = \frac{1}{r\sqrt{\eta_0}} \sum_{\nu} \left[ \mathcal{R}_{\bar{\tau},l}^{(1)} b_{\nu}^{(1)}(t - r/\mathrm{c}) + \mathcal{R}_{\bar{\tau},l}^{(2)} b_{\nu}^{(2)}(t + r/\mathrm{c}) \right] (-1)^{\tau-1} \boldsymbol{A}_{\bar{\nu}}(\hat{\boldsymbol{r}}).$$

Recall that $b_{\nu}^{(j)}(t)$ are assumed to be distributions in general. In the case they are regular functions, the electromagnetic power passing in the negative $r$-direction through a spherical shell of radius $r$ at the time $t$ is

$$\begin{aligned} P(r, t) &= \int_{\Omega_{\hat{\boldsymbol{r}}}} r^2 \, (-\hat{\boldsymbol{r}}) \cdot [\boldsymbol{E}_{\mathrm{T}}(\boldsymbol{r}, t) \times \boldsymbol{H}_{\mathrm{T}}(\boldsymbol{r}, t)] \, \mathrm{d}\Omega_{\hat{\boldsymbol{r}}} \\ &= - \int_{\Omega_{\hat{\boldsymbol{r}}}} r^2 \, \boldsymbol{E}_{\mathrm{T}}(\boldsymbol{r}, t) \cdot [\boldsymbol{H}_{\mathrm{T}}(\boldsymbol{r}, t) \times \hat{\boldsymbol{r}}] \, \mathrm{d}\Omega_{\hat{\boldsymbol{r}}} \\ &= - \int_{\Omega_{\hat{\boldsymbol{r}}}} \left[ \sum_{\nu} \sum_{j=1}^{2} \mathcal{R}_{\tau,l}^{(j)} b_{\nu}^{(j)}(t \mp r/\mathrm{c}) \boldsymbol{A}_{\nu}(\hat{\boldsymbol{r}}) \right] \cdot \left[ \sum_{\nu} \sum_{j=1}^{2} \mathcal{R}_{\bar{\tau},l}^{(j)} b_{\nu}^{(j)}(t \mp r/\mathrm{c}) \boldsymbol{A}_{\nu}(\hat{\boldsymbol{r}}) \right] \mathrm{d}\Omega_{\hat{\boldsymbol{r}}}, \end{aligned}$$

where $\Omega_{\hat{\boldsymbol{r}}} = \{(\theta, \phi) : 0 \leq \theta \leq \pi, 0 \leq \phi \leq 2\pi\}$ is the unit sphere and $\mathrm{d}\Omega_{\hat{\boldsymbol{r}}} = \sin\theta \, \mathrm{d}\theta \, \mathrm{d}\phi$. Here (A.2) has been employed, and the upper (lower) signs are for $j = 1$

$(j = 2)$. The orthogonality relation (A.3) ensures that the two sums over $\nu$ may be replaced by one. Also, all cross-terms in $j$ cancel each other:

$$P(r,t) = -\sum_{\nu}\sum_{j=1}^{2}\left[\mathcal{R}_{\tau,l}^{(j)} b_{\nu}^{(j)}(t \mp r/\mathrm{c})\right]\left[\mathcal{R}_{\bar{\tau},l}^{(j)} b_{\nu}^{(j)}(t \mp r/\mathrm{c})\right].$$

The power $P(r,t)$ may be divided into one radiating part, and another part appertaining to the reactive near-field:

$$P(r,t) = P_{\mathrm{rad}}(r,t) + P_{\mathrm{react}}(r,t), \tag{3.4}$$

where

$$P_{\mathrm{rad}}(r,t) = \sum_{\nu} |b_{\nu}^{(2)}(t + r/\mathrm{c})|^2 - |b_{\nu}^{(1)}(t - r/\mathrm{c})|^2 \tag{3.5}$$

is only dependent on $r$ via $t \mp r/\mathrm{c}$. The reactive power $P_{\mathrm{react}}(r,t)$ tends to zero as $r \to \infty$, and furthermore it has a zero mean for all $r \geq a$, *i.e.*,

$$\int_{-\infty}^{\infty} P_{\mathrm{react}}(r,t)\,\mathrm{d}t = 0. \tag{3.6}$$

This result is derived in [21], where also $P_{\mathrm{rad}}$ and $P_{\mathrm{react}}$ are described in more detail. An illustration of the radiative and reactive power flow for TM-modes of orders $l = 2$ and $l = 5$ can be found in Figure 1 and Figure 2 in [21]. It is made clear there that the reactive power becomes larger for higher order modes if the radiative power is the same.

# 4 The scattering matrix $\tilde{\mathbf{S}}_{\mathrm{S}}$

This section introduces the scattering matrix $\tilde{\mathbf{S}}_{\mathrm{S}}$, which for a given scatterer relates the outgoing wave amplitudes $\tilde{b}_{\nu}^{(1)}(k)$ to the incoming $\tilde{b}_{\nu}^{(2)}(k)$. The equivalent to the scattering matrix in the time domain is also covered. The elements of the scattering matrix are related to passive systems (as described in Section 2.2) in case the scatterer is passive. This is described in more detail below, using the time domain expressions for the vector spherical waves presented in Section 3. Herglotz functions corresponding to (2.6) and their low-frequency expansions of the type (2.1) are derived next. In the end of the section all this is used to obtain sum rules and physical bounds on the diagonal elements of $\tilde{\mathbf{S}}_{\mathrm{S}}$.

Assume that the scatterer is linear, continuous, and time-translational invariant, *i.e.*, that the constitutive relations relating the electric and magnetic flux densities $\boldsymbol{D}(t)$ and $\boldsymbol{B}(t)$ to the electric and magnetic fields $\boldsymbol{E}(t)$ and $\boldsymbol{H}(t)$ are on convolution form, as discussed in Section 2.2. In this case the relation between the outgoing and incoming amplitudes $b_{\nu}^{(1)}(t)$ and $b_{\nu}^{(2)}(t)$ must also be on convolution form, $b_{\nu}^{(1)}(t) = \sum_{\nu'} S_{\nu,\nu'} * b_{\nu'}^{(2)}(t)$. With matrix notation,

$$\boldsymbol{b}^{(1)}(t) = \mathbf{S}_{\mathrm{S}} * \boldsymbol{b}^{(2)}(t), \tag{4.1}$$

where $\boldsymbol{b}^{(1)} = [b_1^{(1)}\ b_2^{(1)} \ldots]^{\mathrm{T}}$ and $\boldsymbol{b}^{(2)}$ is defined analogously. The order of the multi-index is specified in Appendix A.1. In the frequency domain, (4.1) reads

$$\tilde{\boldsymbol{b}}^{(1)}(k) = \tilde{\mathbf{S}}_{\mathrm{S}}(k)\tilde{\boldsymbol{b}}^{(2)}(k), \tag{4.2}$$

where $\tilde{\mathbf{S}}_{\mathrm{S}}(k)$ is the infinite dimensional scattering matrix.

## 4.1 Implications of passivity on $\tilde{\mathbf{S}}_{\mathrm{S}}$

It is now shown that the elements of $\mathbf{S}_{\mathrm{S}}(t-2a/\mathrm{c})$ are the impulse responses of passive systems in case the scatterer is passive; in this case the total radiative power that has passed through a sphere of radius $r \geq a$ before the time $T$ must be non-negative. This means

$$\int_{-\infty}^{T} P_{\mathrm{rad}}(r,t)\,\mathrm{d}t = \int_{-\infty}^{T} \sum_{\nu} |b_\nu^{(2)}(t+r/\mathrm{c})|^2 - |b_\nu^{(1)}(t-r/\mathrm{c})|^2\,\mathrm{d}t \geq 0,$$

for all $T \in \mathbb{R}$ and $r \geq a$, where (3.5) has been used. Recall that it is only necessary to consider smooth, compactly supported incoming wave amplitudes $b_\nu^{(2)} \in \mathcal{D}$, as discussed in Section 2.2. Using (4.1) and letting the incoming field consist of only one vector spherical wave give

$$\int_{-\infty}^{T} P_{\mathrm{rad},\nu'}(r,t)\,\mathrm{d}t = \int_{-\infty}^{T} b_{\nu'}^{(2)}(t+r/\mathrm{c}) - \sum_{\nu} |S_{\nu,\nu'} * b_{\nu'}^{(2)}(t-r/\mathrm{c})|^2\,\mathrm{d}t \geq 0,$$

for all $T \in \mathbb{R}$, $r \geq a$ and $\nu'$. Note that the above energy expression closely resembles that in (2.4), except for the time shifts $-2r/\mathrm{c}$ in the outgoing waves. Hence $S_{\nu,\nu'}(t-2a/\mathrm{c})$ is the impulse response of a passive operator for all $\nu,\nu'$, and so its Fourier-transform $\mathrm{e}^{\mathrm{i}2ka}\tilde{S}_{\nu,\nu'}(k)$ is holomorphic and bounded in magnitude by one for $k \in \mathbb{C}^+$, see Section 2.2 and [2, 25, 29]. Furthermore, $\mathrm{e}^{\mathrm{i}2ka}\tilde{S}_{\nu,\nu'}(k)$ satisfies the symmetry (2.5).

The time shift $-2a/\mathrm{c}$ can be understood intuitively in the sense that the outgoing wave can appear at $r = a$ as soon as the incoming wavefront has reached $r = a$, see Figure 3. This is discussed from a somewhat different perspective in [17].

## 4.2 Low-frequency asymptotic behaviour of $\tilde{\mathbf{S}}_{\mathrm{S}}$

To derive equalities of the type (2.8), the low-frequency asymptotic expansion of the $\tilde{\mathbf{S}}_{\mathrm{S}}$-matrix is required. For this reason, consider the alternative decomposition of the electric field in outgoing and regular vector spherical waves:

$$\widetilde{\boldsymbol{E}}(\boldsymbol{r},k) = k\sqrt{\eta_0}\sum_{\nu} \mathrm{i}^{l+2-\tau}\tilde{d}_\nu^{(1)}(k)\boldsymbol{u}_\nu^{(1)}(k\boldsymbol{r}) + \mathrm{i}^{l+2-\tau}\tilde{d}_\nu^{(v)}(k)\boldsymbol{v}_\nu(k\boldsymbol{r}). \tag{4.3}$$

Here $\boldsymbol{v}_\nu(k\boldsymbol{r})$ denotes regular vector spherical waves, defined as $\boldsymbol{v}_\nu(k\boldsymbol{r}) = (\boldsymbol{u}_\nu^{(1)}(k\boldsymbol{r}) + \boldsymbol{u}_\nu^{(2)}(k\boldsymbol{r}))/2$ (see Appendix A.1). The relation corresponding to (4.2) is $\tilde{\boldsymbol{d}}^{(1)}(k) =$

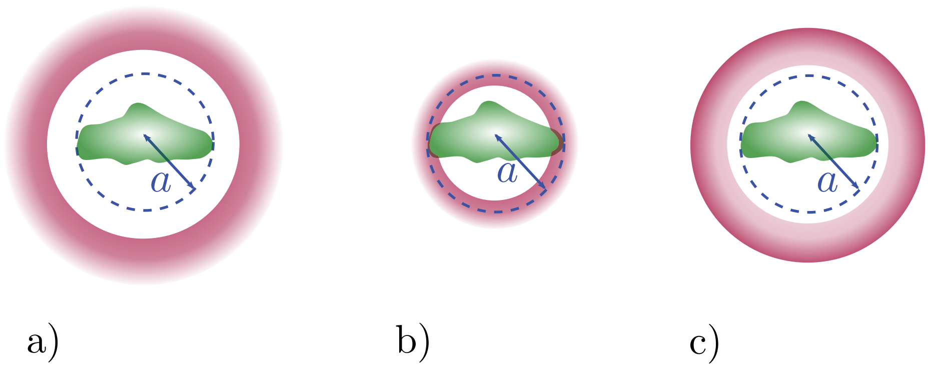


**Figure 3**: An incoming spherical wave $b_{\nu'}^{(2)}(t + r/\mathrm{c})$: a) impinges on the scatterer, b) interacts with the scatterer, and c) creates outgoing waves $\sum_\nu S_{\nu,\nu'} * b_\nu^{(2)}(t - r/\mathrm{c})$. Note that the picture is over-simplified, but it makes it believable that $S_{\nu,\nu'}(t-2a/\mathrm{c})$ is the impulse response of a passive operator for all $\nu$ and $\nu'$.

$\tilde{\mathbf{T}}(k)\tilde{\boldsymbol{d}}^{(v)}(k)$, where $\tilde{\mathbf{T}}$ is the so called transition, or $T-$, matrix. Evidently, $\tilde{\mathbf{S}}_{\mathrm{S}} = 2\tilde{\mathbf{T}} + \mathbf{I}$, where $\mathbf{I}$ is the infinite dimensional identity matrix.

The advantage of a decomposition in regular and outgoing waves is that a plane wave $\widetilde{\boldsymbol{E}}_{\mathrm{i}}$ impinging on the scatterer is regular everywhere, while the produced scattered field $\widetilde{\boldsymbol{E}}_{\mathrm{s}}$ has to satisfy the radiation condition. Accordingly, in this situation $\widetilde{\boldsymbol{E}}_{\mathrm{i}}$ equals the sum over $\boldsymbol{v}_\nu$, while $\widetilde{\boldsymbol{E}}_{\mathrm{s}}$ is the sum over $\boldsymbol{u}_\nu^{(1)}$. Consider a plane wave $\boldsymbol{E}_0(t - \boldsymbol{r}\cdot\hat{\boldsymbol{k}}/\mathrm{c})$ propagating in the $\hat{\boldsymbol{k}}$-direction, corresponding to $\mathrm{e}^{\mathrm{i}\boldsymbol{r}\cdot\boldsymbol{k}}\widetilde{\boldsymbol{E}}_0(k)$ in the frequency domain. Here $\boldsymbol{k} = k\hat{\boldsymbol{k}}$ and as usual $\widetilde{\boldsymbol{E}}_0(k) = (\mathcal{F}\boldsymbol{E}_0)(\omega)$ with $k = \omega/\mathrm{c}$.

The radiating part of the scattered field is described by the far-field amplitude $\boldsymbol{F}$, *viz.*,

$$\boldsymbol{E}_{\mathrm{s}}(t,\boldsymbol{r}) = \frac{\boldsymbol{F}(t - r/\mathrm{c},\hat{\boldsymbol{r}})}{r} + \mathcal{O}(r^{-2}), \quad \widetilde{\boldsymbol{E}}_{\mathrm{s}}(k,\boldsymbol{r}) = \frac{\mathrm{e}^{\mathrm{i}kr}\widetilde{\boldsymbol{F}}(k,\hat{\boldsymbol{r}})}{r} + \mathcal{O}(r^{-2}), \qquad \text{as } r\to\infty. \tag{4.4}$$

Due to the assumption of convolution form for the constitutive relations, a scattering dyadic $\tilde{\mathbf{S}}$ may be defined:

$$\boldsymbol{F}(t,\hat{\boldsymbol{r}}) = \mathbf{S}(\cdot,\hat{\boldsymbol{r}},\hat{\boldsymbol{k}}) * \boldsymbol{E}_0(t), \quad \widetilde{\boldsymbol{F}}(k,\hat{\boldsymbol{r}}) = \tilde{\mathbf{S}}(k,\hat{\boldsymbol{r}},\hat{\boldsymbol{k}})\cdot\widetilde{\boldsymbol{E}}_0(k). \tag{4.5}$$

The elements of the $T$-matrix can be deduced from the scattering dyadic:

$$\tilde{T}_{\nu,\nu'}(k) = \frac{\mathrm{i}k}{4\pi}\int\int \boldsymbol{A}_\nu(\hat{\boldsymbol{r}})\cdot\tilde{\mathbf{S}}(k;\hat{\boldsymbol{r}},\hat{\boldsymbol{k}})\cdot\boldsymbol{A}_{\nu'}(\hat{\boldsymbol{k}})\,\mathrm{d}\Omega_{\hat{\boldsymbol{r}}}\,\mathrm{d}\Omega_{\hat{\boldsymbol{k}}}. \tag{4.6}$$

See Appendix A.2 for details.

Assume that the medium of the scatterer is anisotropic in the static limit ($k = 0$), so that the constitutive relations are

$$\begin{aligned}\widetilde{\boldsymbol{D}}(0,\boldsymbol{r}) &= \epsilon_0\boldsymbol{\epsilon}(0,\boldsymbol{r})\cdot\widetilde{\boldsymbol{E}}(0,\boldsymbol{r})\\ \widetilde{\boldsymbol{B}}(0,\boldsymbol{r}) &= \mu_0\boldsymbol{\mu}(0,\boldsymbol{r})\cdot\widetilde{\boldsymbol{H}}(0,\boldsymbol{r}).\end{aligned}$$

Here $\widetilde{\boldsymbol{D}}(k,\boldsymbol{r})$ denotes the electric flux density and $\widetilde{\boldsymbol{B}}(k,\boldsymbol{r})$ the magnetic flux density at the point $\boldsymbol{r}$ and wavenumber $k$. The relative permittivity and permeability dyadics are denoted $\boldsymbol{\epsilon}(k,\boldsymbol{r})$ and $\boldsymbol{\mu}(k,\boldsymbol{r})$, respectively, and $\epsilon_0$ and $\mu_0$ are the permittivity and permeability of free space, respectively. The low frequency expansion of $\tilde{\mathbf{S}}(k,\hat{\boldsymbol{r}},\hat{\boldsymbol{k}})$ is then

$$\tilde{\mathbf{S}}(k,\hat{\boldsymbol{r}},\hat{\boldsymbol{k}})\cdot\boldsymbol{E}=\frac{k^2}{4\pi}\left\{\hat{\boldsymbol{r}}\times\Big[(\boldsymbol{\gamma}_{\mathrm{e}}\cdot\boldsymbol{E})\times\hat{\boldsymbol{r}}\Big]+\Big[\boldsymbol{\gamma}_{\mathrm{m}}\cdot(\hat{\boldsymbol{k}}\times\boldsymbol{E})\Big]\times\hat{\boldsymbol{r}}\right\}+\mathcal{O}(k^3),\quad\text{as } k\to 0,\tag{4.7}$$

where $\boldsymbol{E}$ is a constant vector. The electric polarizability dyadic $\boldsymbol{\gamma}_{\mathrm{e}}$ relates the electric dipole moment induced in the scatterer to an applied static homogeneous electric field $\widetilde{\boldsymbol{E}}(0)$, *viz.*, $\boldsymbol{p}=\epsilon_0\boldsymbol{\gamma}_{\mathrm{e}}\cdot\widetilde{\boldsymbol{E}}(0)$. Similarly, the magnetic dipole moment induced by an applied static homogeneous magnetic field $\widetilde{\boldsymbol{H}}(0)$ is given by $\boldsymbol{m}=\boldsymbol{\gamma}_{\mathrm{e}}\cdot\widetilde{\boldsymbol{H}}(0)$. The polarizability dyadics are thoroughly discussed in [15] and [23]. Now let $\boldsymbol{E}=\boldsymbol{A}_{\nu'}(\hat{\boldsymbol{k}})$. From (4.6) and (4.7) it follows that

$$\tilde{S}_{\nu,\nu'}(k)=\delta_{\nu,\nu'}+\mathrm{i}2\rho_{\nu,\nu'}k^3a^3+\mathcal{O}(k^4),\quad\text{as } k\to 0,\tag{4.8}$$

where

$$\rho_{\nu,\nu'}=\frac{1}{16\pi^2a^3}\iint\boldsymbol{A}_{\nu}(\hat{\boldsymbol{r}})\cdot\boldsymbol{\gamma}_{\mathrm{e}}\cdot\boldsymbol{A}_{\nu'}(\hat{\boldsymbol{k}})+(-1)^{\tau+\tau'}\boldsymbol{A}_{\bar{\nu}}(\hat{\boldsymbol{r}})\cdot\boldsymbol{\gamma}_{\mathrm{m}}\cdot\boldsymbol{A}_{\bar{\nu}'}(\hat{\boldsymbol{k}})\,\mathrm{d}\Omega_{\hat{\boldsymbol{r}}}\,\mathrm{d}\Omega_{\hat{\boldsymbol{k}}}.$$

Here (A.2) was used, and recall that the dual multi-index is $\bar{\nu}=\{\bar{\tau},s,m,l\}$ with $\bar{\tau}=3-\tau$.

Let $\gamma_{\mathrm{e},xx}=\hat{\boldsymbol{x}}\cdot\boldsymbol{\gamma}_{\mathrm{e}}\cdot\hat{\boldsymbol{x}}$, $\gamma_{\mathrm{e},xy}=\hat{\boldsymbol{x}}\cdot\boldsymbol{\gamma}_{\mathrm{e}}\cdot\hat{\boldsymbol{y}}$ and so on, and use the identities (A.5). This gives explicit expressions for $\rho_{\nu,\nu'}$:

$$\rho_{\nu,\nu'}=\frac{1}{6\pi a^3}\delta_{l,1}\delta_{l',1}\delta_{\tau,\tau'}\gamma_{\{\mathrm{m/e}\},nn'},\tag{4.9}$$

where m (e) should be chosen for $\tau=1$ ($\tau=2$) and

$$n=\begin{cases}x, & \text{for } s=1,\ m=1\\ y, & \text{for } s=2,\ m=1\\ z, & \text{for } s=1,\ m=0,\end{cases}$$

and similarly for $n'$. Note that $\rho_{\nu,\nu'}=0$ for non-dipole modes ($l\geq 2$ or $l'\geq 2$), and that $\rho_{\nu,\nu'}=0$ for $\tau=1$ ($\tau=2$) when the scatterer is non-magnetic (non-electric).

### 4.3 The polarizability dyadics and bounds on $\rho_{\nu,\nu}$

It is clear now that the polarizability dyadics are of vital importance. Until now, the only assumptions made on the constitutive relations of the scatterer is that they are on convolution form in the time domain and passive, and furthermore anisotropic in the static limit. If the scatterer is heterogeneous, these assumptions are made for all points $\boldsymbol{r}$ within the scatterer. It is common to assume that the permittivity and permeability dyadics are symmetric in the static limit, *i.e.*, $\boldsymbol{\epsilon}(0,\boldsymbol{r})=\boldsymbol{\epsilon}(0,\boldsymbol{r})^{\mathrm{T}}$ and

$\boldsymbol{\mu}(0,\boldsymbol{r}) = \boldsymbol{\mu}(0,\boldsymbol{r})^{\mathrm{T}}$. This implies that the polarizability dyadics are also symmetric [23], and hence diagonal for a suitable choice of coordinates. Closed form expressions for the polarizability dyadics exists for anisotropic homogeneous spheroidal scatterers, see [23] and references therein. For the simple case of an isotropic sphere of radius $a$, they are

$$\boldsymbol{\gamma}_{\mathrm{e}} = 4\pi a^3 \frac{\epsilon(0)-1}{\epsilon(0)+2}\,\mathbf{I}$$
$$\boldsymbol{\gamma}_{\mathrm{m}} = 4\pi a^3 \frac{\mu(0)-1}{\mu(0)+2}\,\mathbf{I},$$

where $\mathbf{I}$ is the identity dyadic.

Furthermore, under the assumption of symmetry it can be shown that $\boldsymbol{\gamma}_{\mathrm{e}}$ and $\boldsymbol{\gamma}_{\mathrm{m}}$ are non-decreasing as functions of $\boldsymbol{\epsilon}(0,\boldsymbol{r})$ and $\boldsymbol{\mu}(0,\boldsymbol{r})$ [22]. More specifically, consider two objects with permittivity $\boldsymbol{\epsilon}(0,\boldsymbol{r})$ and $\boldsymbol{\epsilon}'(0,\boldsymbol{r})$, respectively. If $\boldsymbol{\epsilon}'(0,\boldsymbol{r}) - \boldsymbol{\epsilon}(0,\boldsymbol{r})$ is a positive semidefinite dyadic for all $\boldsymbol{r}$ in the object, then $\boldsymbol{\gamma}'_{\mathrm{e}} - \boldsymbol{\gamma}_{\mathrm{e}}$ is positive semidefinite as well. The same holds for $\boldsymbol{\gamma}_{\mathrm{m}}$, with $\boldsymbol{\epsilon}(0,\boldsymbol{r})$ replaced by $\boldsymbol{\mu}(0,\boldsymbol{r})$. The diagonal elements of $\boldsymbol{\gamma}_{\mathrm{e}}$ and $\boldsymbol{\gamma}_{\mathrm{m}}$ for any scatterer (satisfying the aforementioned assumptions) contained in the sphere of radius $a$ are therefore bounded by $4\pi a^3$ for the high contrast sphere. Following (4.9), the parameters $\rho_{\nu,\nu}$ are non-decreasing as functions of $\boldsymbol{\epsilon}(0,\boldsymbol{r})$ and $\boldsymbol{\mu}(0,\boldsymbol{r})$, and thus bounded from above by $\rho_{\nu,\nu} = 2/3$.

If the scatterer is contained within a non-spherical geometry, the diagonal elements of $\boldsymbol{\gamma}_{\mathrm{e}}$ and $\boldsymbol{\gamma}_{\mathrm{m}}$ are bounded by the largest eigenvalue $\gamma_1 \leq 4\pi a^3$ of the high-contrast polarizability dyadic $\boldsymbol{\gamma}_\infty$ of that geometry. Therefore a sharper bound on $\rho_{\nu,\nu}$, given by $\rho_{\nu,\nu} \leq \gamma_1/(6\pi a^3) \leq 2/3$, can be determined. The high-contrast polarizability dyadics $\boldsymbol{\gamma}_\infty$ of many geometries can be calculated numerically, see [10] for some examples.

A widely used material model is the perfect electric conductor (PEC). For a PEC inclusion, $\epsilon(0) = \infty$ and $\mu(0) = 0$. Consequently, $\boldsymbol{\gamma}_{\mathrm{e}}$ ($\boldsymbol{\gamma}_{\mathrm{m}}$) is non-decreasing (non-increasing) as the volume of the PEC inclusion increases [22].

## 4.4 Sum rules and physical limitations on $\tilde{\mathbf{S}}_{\mathrm{S}}$

Now it has been shown that $\mathrm{e}^{\mathrm{i}2ka}\tilde{S}_{\nu,\nu'}(k)$ is a holomorphic function bounded in magnitude by one in $\mathbb{C}^+$ for all $\nu$ and $\nu'$, due to the passivity assumption. Furthermore, its low frequency asymptotic expansion has been determined in (4.8) and (4.9). It remains to define a Herglotz function and derive sum rules of the type (2.8). The Herglotz function corresponding to (2.6) is

$$h_{\nu,\nu'}(k) = -\mathrm{i}\log\left(\frac{\mathrm{e}^{\mathrm{i}2ka}\tilde{S}_{\nu,\nu'}(k)}{B_{\nu,\nu'}(k)}\right).$$

Here $B_{\nu,\nu'}$ is a Blaschke products of the form (2.7) for each pair $(\nu,\nu')$. Since $\mathrm{e}^{\mathrm{i}2ka}\tilde{S}_{\nu,\nu}(k) \to 1$ as $k \to 0$ when $\tilde{S}_{\nu,\nu}$ is a diagonal element of the scattering matrix, the low-frequency expansion may be calculated separately for that factor and the

Blaschke product (*cf.*, [2]):

$$h_{\nu,\nu}(k) = 2ka + 2\rho_{\nu,\nu}k^3a^3 + \mathcal{O}(k^4) + 2\sum_n \sum_{q=1,3,\ldots}^{\infty} \frac{k^q}{q}\,\mathrm{Im}\,\frac{1}{k_n^q}, \quad \text{as } k \to 0. \tag{4.10}$$

This is not necessarily possible for the off diagonal terms $h_{\nu,\nu'}$, where $\nu \neq \nu'$, since then $\tilde{S}_{\nu,\nu'}(k)$ tends to zero as $k \to 0$. Only terms with odd $q$ appear in (4.10) due to the symmetry (2.5).

Note that the low-frequency asymptotic expansions (4.7) and (4.10) are valid as $k \to 0$ for all arguments of $k$, and especially as $k \hat{\to} 0$. With the notation of Section 2.1, $N = 2$ and hence two sum rules of the type (2.8) (using $p = 1, 2$) can be deduced:

$$\lim_{\varepsilon\to0^+}\lim_{k''\to0^+}\frac{1}{\pi}\int_\varepsilon^\infty \frac{1}{k'^2}\ln\frac{1}{|\tilde{S}_{\nu,\nu}(k'+\mathrm{i}k'')|}\,\mathrm{d}k' = a - \frac{\beta_{\nu,\nu}}{2} + \sum_n \mathrm{Im}\,\frac{1}{k_n} \tag{4.11}$$

and

$$\lim_{\varepsilon\to0^+}\lim_{k''\to0^+}\frac{1}{\pi}\int_\varepsilon^\infty \frac{1}{k'^4}\ln\frac{1}{|\tilde{S}_{\nu,\nu}(k'+\mathrm{i}k'')|}\,\mathrm{d}k' = a^3\rho_{\nu,\nu} + \frac{1}{3}\sum_n \mathrm{Im}\,\frac{1}{k_n^3}. \tag{4.12}$$

Here $k' = \mathrm{Re}\,k$ and $k'' = \mathrm{Im}\,k$, in consistency with previous notation. As discussed in Section 2.1, the left-hand sides may be interpreted as integrals of $-\ln|\tilde{S}_{\nu,\nu}(k')|/k'^{2p}$ in the distributional sense, *i.e.*, contributions from possible singularities in the interval $(0,\infty)$ should be included.

Both sum rules incorporate the radius $a$ of the circumscribing sphere, and the second depends on the material and shape of the scatterer via $\rho_{\nu,\nu}$ given by (4.9). The parameter $\beta_{\nu,\nu} = \lim_{k\hat{\to}\infty} h_{\nu,\nu}(k)/k$ is greater than or equal to zero. Evidently, $\beta_{\nu,\nu} > 0$ applies if the chosen circumscribing sphere is larger than the smallest circumscribing sphere, but it is expected that $\beta_{\nu,\nu} = 0$ if $a$ is chosen as small as possible. This is true for isotropic spherical scatterers with material described by *e.g.*, the Debye or Lorentz models. It is hard to prove this statement for an arbitrary scatterer, so it is assumed that $\beta_{\nu,\nu}$ can be larger than zero.

In order to derive physical limitations, consider a finite wavenumber interval, $\mathcal{K} = [k_0(1-B_K/2), k_0(1+B_K/2)]$, with center wavenumber $k_0$ and fractional bandwidth $B_K < 2$. Letting $S_0 = \sup_{k'\in\mathcal{K}}|\tilde{S}_{\nu,\nu}(k')|$, it follows that[3]

$$\frac{B_K \ln S_0^{-1}}{\pi} \leq k_0 a + \sum_n \mathrm{Im}\,\frac{k_0}{k_n} \tag{4.13}$$

and

$$\frac{B_K \ln S_0^{-1}}{\pi} \leq k_0^3 a^3 \rho_{\nu,\nu} + \frac{1}{3}\sum_n \mathrm{Im}\,\frac{k_0^3}{k_n^3}. \tag{4.14}$$

[3]Here $S_0 = \sup_{k'\in\mathcal{K}}|\tilde{S}_{\nu,\nu}(k')|$ should be interpreted as the supremum over those $k' \in \mathcal{K}$ such that $\tilde{S}_{\nu,\nu}(k')$ is well-defined (recall that it is well-defined for almost all $k' \in \mathbb{R}$). Also note here that the inequalities (4.13)–(4.14) are valid even if (4.11)–(4.12) must be interpreted as (2.9).

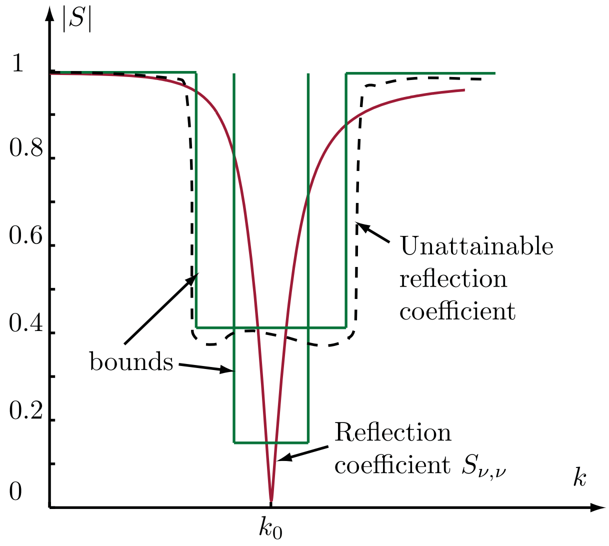


**Figure 4**: Interpretation of the bound (4.15). In the figure, bounds for a given center wavenumber $k_0$ are depicted for two different values of $S_0$ (and thus two different values of $B_K$). The bound states that the magnitude of all reflection coefficients $S_{\nu,\nu}$ have to intersect the boxes, when the scatterer satisfies the aforementioned assumptions; also shown in the figure is one attainable and one unattainable reflection coefficient.

Here it has been used that $k_0^{2p-1}\int_{\mathcal{K}} 1/k^{2p}\,\mathrm{d}k \geq B_K$ for $p = 0, 1, \ldots$ Note also that $k_0^{2p-1}\int_{\mathcal{K}} 1/k^{2p}\,\mathrm{d}k \approx B_K$ when $B_K \ll 1$.

The sum in the right-hand side of (4.13) is non-positive (since $\operatorname{Im} k_n > 0$ for all $k_n$), and so

$$\frac{B_K \ln S_0^{-1}}{\pi} \leq k_0 a.$$

An alternative bound not containing the sum over all zeros can also be derived (see Appendix A.3):

$$\begin{aligned}\frac{B_K \ln S_0^{-1}}{\pi} &\leq k_0 a - \sqrt[3]{\iota + \zeta} + \sqrt[3]{\iota - \zeta} \\ &= \left(\frac{1}{3} + \rho_{\nu,\nu}\right)\left(k_0^3 a^3 - k_0^5 a^5\right) + \mathcal{O}(k_0^7), \qquad \text{as } k_0 \to 0.\end{aligned} \tag{4.15}$$

Here the material and geometry of the scatterer are contained in $\rho_{\nu,\nu}$ via $\zeta = 3k_0 a(1 - \rho_{\nu,\nu} k_0^2 a^2)/2$ and $\iota = \sqrt{1 + \zeta^2}$. The term $k_0^3 a^3/3$ in the bound stems from the circumscribing sphere. The bound (4.15) states that, somewhere on the wavenumber interval $\mathcal{K}$, the reflection coefficient $\tilde{S}_{\nu,\nu}(k')$ for mode $\nu$ must be larger in magnitude than some value prescribed by the fractional bandwidth $B_K$, the radius of the smallest circumscribing sphere $a$, and the material properties of the scatterer via $\rho_{\nu,\nu}$, see Figure 4.

An interpretation of the bound is as a limitation on the absorption of a vector spherical wave over a bandwidth. To see this, consider the total energy $e(\infty)$ absorbed by the scatterer when the incoming field consists of only the mode $\nu'$, and $b^{(2)}_{\nu'}(t)$ is assumed to be in $\mathrm{L}^2$. By (3.4)–(3.6), it is (with $r \geq a$)

$$e(\infty) = \int_{-\infty}^{\infty} P_{\nu'}(r,t)\,\mathrm{d}t = \int_{-\infty}^{\infty} P_{\mathrm{rad},\nu'}(r,t)\,\mathrm{d}t = \int_{-\infty}^{\infty} |b^{(2)}_{\nu'}(t)|^2 - \sum_{\nu} |S_{\nu,\nu'} * b^{(2)}_{\nu'}(t)|^2\,\mathrm{d}t.$$

The expression for $e(\infty)$ may be rewritten with Parseval's equation:

$$e(\infty) = \frac{1}{2\pi\mathrm{c}} \int_{-\infty}^{\infty} |\tilde{b}^{(2)}_{\nu'}(k')|^2 \left(1 - \sum_{\nu} |\tilde{S}_{\nu,\nu'}(k')|^2\right) \mathrm{d}k'.$$

Hence $1 - \sum_{\nu} |\tilde{S}_{\nu,\nu'}(k')|^2$ is the normalised energy of the incoming mode $\nu'$ that is absorbed by the scatterer at wavenumber $k'$; all of the incoming energy is absorbed if $\sum_{\nu} |\tilde{S}_{\nu,\nu'}(k')|^2 = 0$, while no energy is absorbed in the case $\sum_{\nu} |\tilde{S}_{\nu,\nu'}(k')|^2 = 1$. The absorbed normalised energy is obviously less than or equal to $1 - |\tilde{S}_{\nu,\nu}(k')|^2$. Also recall that $\tilde{S}_{\nu,\nu'}(k') \to 0$, as $k' \to 0$, when $\nu \neq \nu'$, due to (4.8).

# 5 Examples

## 5.1 Nanoshells

A nanoshell is a dielectric core covered by a thin coat of metal. By varying the core radius, shell thickness, and materials, they can be constructed to scatter or absorb large parts of incoming electromagnetic waves in the visible light and near-infrared (NIR) spectra. Applications include *e.g.*, biomedical imaging and treatment of tumours.

In cancer treatment, the nanoshells are shuttled into the tumour using a so called "Trojan horse"-method [4]. Hereafter they are illuminated by laser light, causing most of the cancer cells to die, see Figure 1 in [4]. It is thus desirable to design nanoshells that absorb large parts of the laser energy. In [4, 18], the nanoshells are spherical cores of silicon dioxide ($\mathrm{SiO_2}$) covered with gold. The radius of the core is typically around 60 nm, and the gold shell is $5-20$ nm thick. The bound in (4.15) is well suited to study this problem, since the normalised absorbed energy from mode $\nu$ is bounded by $1 - |\tilde{S}_{\nu,\nu}|^2$ as discussed in Section 4.4. An illustration can be found in Figure 5.

## 5.2 Physical limitations on antennas

As discussed in Section 4.4, (4.15) places a bound on the absorption of a spherical wave over a bandwidth, which makes it a good candidate to find limits on the performance of antennas. Furthermore, the communications channels of multiple-input multiple-output (MIMO) antenna systems are coupled to orthogonal sets of vector spherical waves [7]. It is unusual to compute the $\tilde{\mathbf{S}}_{\mathrm{S}}$-matrix elements of an antenna. Instead, consider the setup depicted in Figure 6. The antenna is fed the power $P_{\mathrm{in}}(k)$ by a transmission line, and a matching network is employed in order

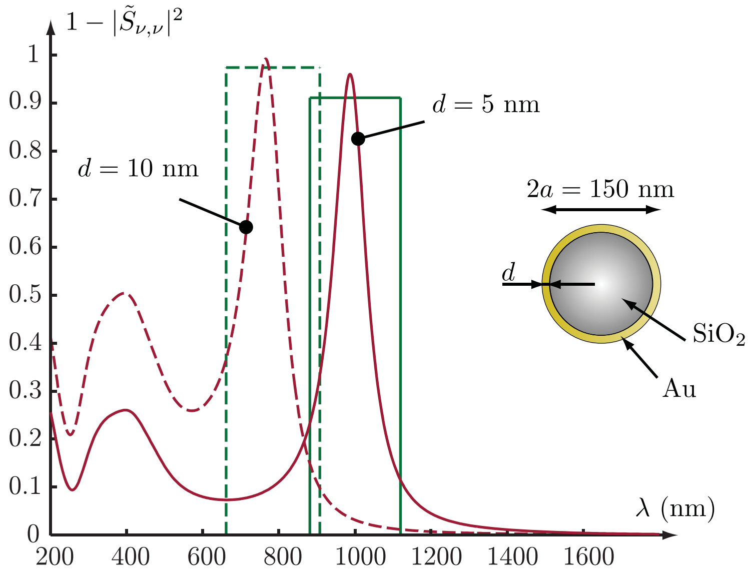


**Figure 5**: The reflection coefficient $\tilde{S}_{\nu,\nu}$ of the electric dipole modes ($\tau = 2, l = 1$) for a nanoshell of outer radius $a = 75\,\text{nm}$, consisting of a spherical silicon dioxide core covered by a layer of gold of thickness $d = 5$ and $10\,\text{nm}$, respectively. Here $\lambda$ denotes the wavelength. The bound is (4.15) with $\rho_{\nu,\nu} = 2/3$, and it states that the curves have to intersect the boxes. The reflection coefficient $\tilde{S}_{\nu,\nu}$ was calculated from the closed form expression, using a Matlab-script for a Lorentz-Drude model for gold by Ung et al. [24]. Silicon dioxide is modeled as having negligible losses and a refractive index of $n \approx 1.5$, which is a good model at least for wavelengths 400–1100 nm [14].

to minimise the reflection coefficient $\Gamma(k)$. The power rejected due to mismatch is $|\Gamma(k)|^2 P_{\text{in}}(k)$, and obviously the radiated power is bounded as

$$P_{\text{rad}}(k) \leq (1 - |\Gamma(k)|^2) P_{\text{in}}(k),$$

with equality if there are no ohmic losses in the antenna.

Many antennas can be modeled by the resonance circuit in Figure 7 in a frequency interval close to their respective resonance frequencies [9]. Here the quality factor is

$$Q = k_0 \mathrm{c} \frac{Z'(k_0)}{2R}, \tag{5.1}$$

where $k_0$ is the resonance wavenumber of the antenna, $Z$ its input impedance, and $R = Z(k_0)$ the (real-valued) input impedance at the resonance. A prime denotes differentiation with respect to the argument. Using Fano's bounds on optimal matching [6], it is straightforward to show that [9]

$$\frac{B_K \ln \Gamma_0^{-1}}{\pi} \leq \frac{1}{Q}, \tag{5.2}$$

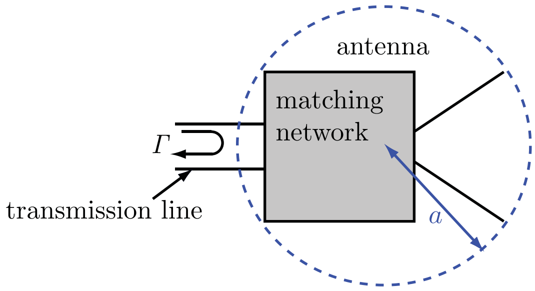


**Figure 6**: The antenna and matching network considered in Example 5.2.

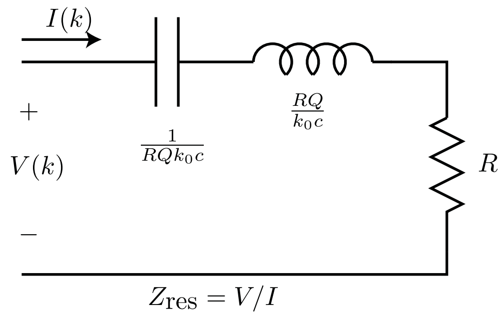


**Figure 7**: For many antennas, the impedance $Z_{\text{res}}(k)$ of the resonance circuit is a good approximation for the antenna input impedance $Z(k)$ close to its resonance wavenumber $k_0$ [9]. The quality factor $Q$ is given by (5.1).

applies whatever the matching network is. Here $\Gamma_0 = \max_{k\in\mathcal{K}} |\Gamma(k)|$. The wavenumber interval is $\mathcal{K} = [k_0(1 - B_K/2), k_0(1 + B_K/2)]$, with center wavenumber $k_0$ and fractional bandwidth $B_K$.

The input impedance $Z(k)$ of an antenna, and hence also the quality factor $Q$ in (5.1), may be calculated numerically. Equation (5.2) provides a means to compare the bound (4.15) to the quality factor of an antenna; since $1 - |\Gamma|^2$ places a bound on the radiated power in terms of the input power, and $1 - |S_{\nu,\nu}|$ limits the absorbed power from a single mode $\nu$, $\Gamma$ and $S_{\nu,\nu}$ are on equal footing. In Figure 8, the bound in (4.15) is compared to the inverse of the numerically determined quality factor $Q$ of four wire antennas.

# 6 Conclusions

Electromagnetic waves may be scattered and/or absorbed when they interact with various objects. Understanding this interaction is vital in many applications, from classical optics to antenna theory. One way to analyse it is to apply physical limitations to it; in essence, the physical limitations state what can and cannot be expected from a certain physical system.

There are several publications addressing physical limitations in scattering and

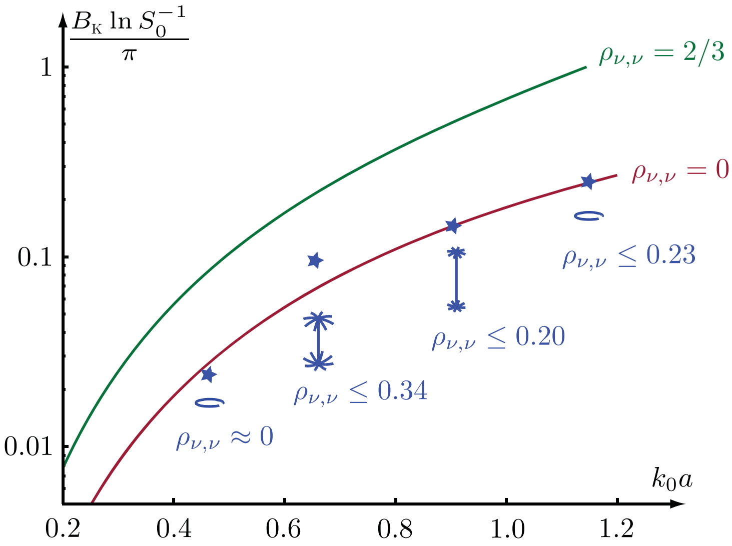


**Figure 8**: The lines are the bound (4.15) for $\rho = 2/3$ and $\rho = 0$, respectively. Four wire antennas were used in the example, with wires modeled as perfect electric conductors of diameter 2 mm. The radii of the loops are 60 mm (giving $a = 62$ mm), and the heights of the umbrellas are 100 mm (so that $a = 52$ mm). Here $a$ is the radius of the smallest circumscribing sphere. The loop with resonance at $k_0 a \approx 0.46$ is in series with a 100 F capacitance, causing it to radiate much like a pure magnetic dipole close to the resonance. The input impedances and resonance wavenumbers for the antennas were calculated using the commercial software E-Field (http://www.efieldsolutions.com). The inverse of $Q$ given by (5.1) is depicted for the four antennas at their respective resonance wavenumbers $k_0$. The electric polarizability dyadics $\boldsymbol{\gamma}_\mathrm{e}$ were calculated using a Method of Moments code, and from them the bounds on $\rho_{\nu,\nu}$ shown in the figure could be determined.

antenna theory, see *e.g.*, [3, 5, 8, 12, 19, 23]. However, the present paper seems to be the first to derive physical limitations on the scattering of electromagnetic vector spherical waves. The vector spherical waves constitute a means to expand a given electromagnetic wave in orthogonal waves, and are commonly used [11, 20, 21]. In wireless communication, they are intimately linked to the orthogonal communication channels of multiple-input multiple-output (MIMO) systems [7].

The derivation makes use of a general approach to obtain sum rules and physical limitations on passive physical systems on convolution form presented in [2]. The limitations in this paper are valid for all heterogeneous passive scatterers with constitutive relations on convolution form in the time domain, and anisotropic in the static limit. They state that the reflection coefficients cannot be arbitrarily small over a whole wavenumber interval; how small is determined by the center wavenumber and fractional bandwidth, the radius of the smallest sphere circumscribing the scatterer, and its static material properties.

The bounds can be interpreted as limits on the absorption of power from the respective modes. They are particularly useful for the electrically small scatterers, and can therefore be employed to analyse sub-wavelength structures designed to be resonant in one or more frequency bands. Two examples are nanoshells and antennas, discussed in the examples in this paper.

# Acknowledgments

The financial support by the High Speed Wireless Communications Center of the Swedish Foundation for Strategic Research (SSF) is gratefully acknowledged.

# Appendix Appendix

## A.1 Definition of vector spherical waves

The incoming ($j = 2$) and outgoing ($j = 1$) vector spherical waves [11] are defined as

$$\begin{cases} \boldsymbol{u}^{(j)}_{1sml}(k\boldsymbol{r}) = \mathrm{h}^{(j)}_l(kr)\boldsymbol{A}_{1sml}(\hat{\boldsymbol{r}}) \\ \boldsymbol{u}^{(j)}_{2sml}(k\boldsymbol{r}) = \dfrac{(kr\mathrm{h}^{(j)}_l(kr))'}{kr}\boldsymbol{A}_{2sml}(\hat{\boldsymbol{r}}) + \sqrt{l(l+1)}\dfrac{\mathrm{h}^{(j)}_l(kr)}{kr}\boldsymbol{A}_{3sml}(\hat{\boldsymbol{r}}). \end{cases} \tag{A.1}$$

Here $\mathrm{h}^{(j)}_l$ denotes the spherical Hankel function of the $j$:th kind and order $l$, and a prime denotes differentiation with respect to the argument $kr$. The regular vector spherical waves $\boldsymbol{v}_\nu$ are almost identical; for them the spherical Hankel functions have been replaced by spherical Bessel functions $\mathrm{j}_l = (\mathrm{h}^{(1)}_l + \mathrm{h}^{(2)}_l)/2$. The vector spherical harmonics $\boldsymbol{A}_{\tau sml}$ are defined by

$$\begin{cases} \boldsymbol{A}_{1sml}(\hat{\boldsymbol{r}}) = \dfrac{1}{\sqrt{l(l+1)}}\nabla \times (\boldsymbol{r}Y_{sml}(\hat{\boldsymbol{r}})) \\ \boldsymbol{A}_{2sml}(\hat{\boldsymbol{r}}) = \dfrac{1}{\sqrt{l(l+1)}}r\nabla Y_{sml}(\hat{\boldsymbol{r}}) \\ \boldsymbol{A}_{3sml}(\hat{\boldsymbol{r}}) = \hat{\boldsymbol{r}}Y_{sml}(\hat{\boldsymbol{r}}). \end{cases}$$

Here $Y_{sml}$ are the (scalar) spherical harmonics

$$Y_{sml}(\theta,\phi) = -\sqrt{\frac{2-\delta_{m0}}{2\pi}}\sqrt{\frac{2l+1}{2}\frac{(l-m)!}{(l+m)!}}P^m_l(\cos\theta)\left\{\begin{matrix}\cos m\phi \\ \sin m\phi\end{matrix}\right\}$$

and $P^m_l$ are associated Legendre polynomials [1]. The polar angle is denoted $\theta$ while $\phi$ is the azimuth angle. The upper (lower) expression is for $s = 1$ ($s = 2$), and the range of the indices are $l = 1, 2, \dots$ , $m = 0, 1, \dots, l$, $\tau = 1, 2$, $s = 1$ when $m = 0$ and $s = 1, 2$ otherwise. The multi-index $\nu = \{\tau, s, m, l\}$ is introduced to simplify the notation. It is ordered such that $\nu = 2(l^2 + l - 1 + (-1)^s m) + \tau$.

Note that

$$\begin{cases} \hat{\boldsymbol{r}} \cdot \boldsymbol{A}_{1sml}(\hat{\boldsymbol{r}}) = \hat{\boldsymbol{r}} \cdot \boldsymbol{A}_{2sml}(\hat{\boldsymbol{r}}) = 0 \\ \hat{\boldsymbol{r}} \times \boldsymbol{A}_{3sml}(\hat{\boldsymbol{r}}) = \boldsymbol{0}, \end{cases}$$

for which reason $\tau = 1$ (odd $\nu$) identifies a TE mode (magnetic $2^l$-pole) while $\tau = 2$ (even $\nu$) identifies a TM mode (electric $2^l$-pole) when the electric and magnetic fields are defined by (3.1) and (3.2), respectively. Furthermore,

$$\begin{cases} \boldsymbol{A}_{1sml}(\hat{\boldsymbol{r}}) = \boldsymbol{A}_{2sml}(\hat{\boldsymbol{r}}) \times \hat{\boldsymbol{r}} \\ \boldsymbol{A}_{2sml}(\hat{\boldsymbol{r}}) = \hat{\boldsymbol{r}} \times \boldsymbol{A}_{1sml}(\hat{\boldsymbol{r}}). \end{cases} \tag{A.2}$$

The vector spherical harmonics are orthonormal on the unit sphere. More specifically, they satisfy

$$\int_{\Omega_{\hat{\boldsymbol{r}}}} \boldsymbol{A}_{\nu}(\hat{\boldsymbol{r}}) \cdot \boldsymbol{A}_{\nu'}(\hat{\boldsymbol{r}}) \, \mathrm{d}\Omega_{\hat{\boldsymbol{r}}} = \delta_{\nu,\nu'}, \tag{A.3}$$

where $\Omega_{\hat{\boldsymbol{r}}} = \{(\theta, \phi) : 0 \leq \theta \leq \pi, 0 \leq \phi \leq 2\pi\}$ is the unit sphere and $\mathrm{d}\Omega_{\hat{\boldsymbol{r}}} = \sin\theta \, \mathrm{d}\theta \, \mathrm{d}\phi$. Define the $\mathrm{L}^2$-norm $|| \cdot ||$ for vector-valued functions on $\Omega_{\hat{\boldsymbol{r}}}$:

$$||\boldsymbol{G}||^2 = \int_{\Omega_{\hat{\boldsymbol{r}}}} \boldsymbol{G}(\hat{\boldsymbol{r}}) \cdot \boldsymbol{G}^*(\hat{\boldsymbol{r}}) \, \mathrm{d}\Omega_{\hat{\boldsymbol{r}}}.$$

If the norm of $\boldsymbol{G}$ is finite, it may be expanded in vector spherical harmonics:

$$\boldsymbol{G}(\hat{\boldsymbol{r}}) = \sum_{\nu} c_{\nu} \boldsymbol{A}_{\nu}(\hat{\boldsymbol{r}}), \tag{A.4}$$

where the coefficients $c_{\nu}$ are given by

$$c_{\nu} = \int_{\Omega_{\hat{\boldsymbol{r}}}} \boldsymbol{G}(\hat{\boldsymbol{r}}) \cdot \boldsymbol{A}_{\nu}(\hat{\boldsymbol{r}}) \, \mathrm{d}\Omega_{\hat{\boldsymbol{r}}},$$

and the sum in the right hand side of (A.4) converges in the norm $|| \cdot ||$.

The following expressions for the Cartesian unit vectors are used in (4.9):

$$\begin{cases} \hat{\boldsymbol{x}} = \sqrt{\dfrac{4\pi}{3}} \boldsymbol{A}_{3e11}(\hat{\boldsymbol{r}}) + \sqrt{\dfrac{8\pi}{3}} \boldsymbol{A}_{2e11}(\hat{\boldsymbol{r}}) \\ \hat{\boldsymbol{y}} = \sqrt{\dfrac{4\pi}{3}} \boldsymbol{A}_{3o11}(\hat{\boldsymbol{r}}) + \sqrt{\dfrac{8\pi}{3}} \boldsymbol{A}_{2o11}(\hat{\boldsymbol{r}}) \\ \hat{\boldsymbol{z}} = \sqrt{\dfrac{4\pi}{3}} \boldsymbol{A}_{3e01}(\hat{\boldsymbol{r}}) + \sqrt{\dfrac{8\pi}{3}} \boldsymbol{A}_{2e01}(\hat{\boldsymbol{r}}). \end{cases} \tag{A.5}$$

There are expansions for the Hankel functions, used to determine the polynomials $R^{(j)}_{\tau,l}$ in (3.3):

$$\begin{cases} h_l^{(1)}(z) = \dfrac{\mathrm{e}^{\mathrm{i}z}}{\mathrm{i}^{l+1} z} \displaystyle\sum_{n=1}^{l} \dfrac{(l+n)!}{n!(l-n)!} (-2\mathrm{i}z)^{-k} \\ h_l^{(2)}(z) = \dfrac{\mathrm{i}^{l+1} \mathrm{e}^{-\mathrm{i}z}}{z} \displaystyle\sum_{n=1}^{l} \dfrac{(l+n)!}{n!(l-n)!} (2\mathrm{i}z)^{-k}. \end{cases} \tag{A.6}$$

## A.2 Derivation of (4.6)

The scattered field $\widetilde{\boldsymbol{E}}_\mathrm{s}$ is the sum over $\boldsymbol{u}_\nu^{(1)}$ in (4.3), *viz.*,

$$\widetilde{\boldsymbol{E}}_\mathrm{s}(k,\boldsymbol{r}) = \sqrt{\eta_0}\sum_\nu \tilde{d}_\nu^{(1)}(k)\boldsymbol{A}_\nu(\hat{\boldsymbol{r}})\frac{\mathrm{e}^{ikr}}{r}\left(1+\mathcal{O}(r^{-1})\right), \qquad \text{as } r\to\infty,$$

where (A.1) and (A.6) have been used. From the above equation it is clear that the far-field amplitude $\widetilde{\boldsymbol{F}}(k,\hat{\boldsymbol{r}})$ in (4.4) is given by

$$\widetilde{\boldsymbol{F}}(k,\hat{\boldsymbol{r}}) = \sqrt{\eta_0}\sum_\nu \tilde{d}_\nu^{(1)}(k)\boldsymbol{A}_\nu(\hat{\boldsymbol{r}}).$$

Using (4.5), multiplying with $\boldsymbol{A}_{\nu'}(\hat{\boldsymbol{r}})$ and integrating over the unit sphere yield

$$\int \boldsymbol{A}_{\nu'}(\hat{\boldsymbol{r}})\cdot\tilde{\mathbf{S}}(k,\hat{\boldsymbol{r}},\hat{\boldsymbol{k}})\cdot\widetilde{\boldsymbol{E}}_0(k)\,\mathrm{d}\Omega_{\hat{\boldsymbol{r}}} = \sqrt{\eta_0}\tilde{d}_{\nu'}^{(1)}(k), \tag{A.7}$$

due to (A.3).

The coefficients $\tilde{d}_{\nu'}^{(1)}(k)$ are given by

$$\sqrt{\eta_0}\tilde{d}_{\nu'}^{(1)}(k) = \sqrt{\eta_0}\sum_{\nu''}\tilde{T}_{\nu',\nu''}(k)\tilde{d}_{\nu''}^{(v)}(k) = \frac{4\pi}{\mathrm{i}k}\sum_{\nu''}\tilde{T}_{\nu',\nu''}(k)\widetilde{\boldsymbol{E}}_0(k)\cdot\boldsymbol{A}_{\nu''}(\hat{\boldsymbol{k}}),$$

where the expansion coefficients $\tilde{d}_{\nu''}^{(v)}(k)$ of a plane wave $\mathrm{e}^{\mathrm{i}\boldsymbol{r}\cdot\boldsymbol{k}}\widetilde{\boldsymbol{E}}_0(k)$ have been used. Inserting this into (A.7) gives

$$\int \boldsymbol{A}_{\nu'}(\hat{\boldsymbol{r}})\cdot\tilde{\mathbf{S}}(k,\hat{\boldsymbol{r}},\hat{\boldsymbol{k}})\cdot\widetilde{\boldsymbol{E}}_0(k)\,\mathrm{d}\Omega_{\hat{\boldsymbol{r}}} = \frac{4\pi}{\mathrm{i}k}\sum_{\nu''}\tilde{T}_{\nu',\nu''}(k)\widetilde{\boldsymbol{E}}_0(k)\cdot\boldsymbol{A}_{\nu''}(\hat{\boldsymbol{k}}),$$

which must be valid for all $\hat{\boldsymbol{k}}$ and $\widetilde{\boldsymbol{E}}_0$. Letting $\widetilde{\boldsymbol{E}}_0(k,\hat{\boldsymbol{k}}) = \boldsymbol{A}_{\nu'''}(\hat{\boldsymbol{k}})\varphi(k)$ for some $\varphi\in\mathcal{S}$ and integrating once more over the unit sphere leads to

$$\int\int \boldsymbol{A}_{\nu'}(\hat{\boldsymbol{r}})\cdot\tilde{\mathbf{S}}(k,\hat{\boldsymbol{r}},\hat{\boldsymbol{k}})\cdot\boldsymbol{A}_{\nu'''}(\hat{\boldsymbol{k}})\varphi(k)\,\mathrm{d}\Omega_{\hat{\boldsymbol{r}}}\,\mathrm{d}\Omega_{\hat{\boldsymbol{k}}} = \frac{4\pi}{\mathrm{i}k}\tilde{T}_{\nu',\nu'''}(k)\varphi(k),$$

and (4.6) is proven.

## A.3 Derivation of (4.15)

First set $k_0/k_n = \theta_n' - i\theta_n''$, where $\theta_n'\in\mathbb{R}$ and $\theta_n''>0$. With $\theta_0 = \sum_n\theta_n''$, (4.13) takes the form

$$\frac{B_K\ln S_0^{-1}}{\pi} \le k_0 a - \theta_0. \tag{A.8}$$

Furthermore, it follows that $\sum_n \operatorname{Im} k_0^3/k_n^3 \le \sum_n \theta_n''^3 \le \theta_0^3$, since

$$\operatorname{Im}\frac{k_0^3}{k_n^3} = \frac{k_0^3}{|k_n|^6}\left[(\operatorname{Im}k_n)^3 - (\operatorname{Re}k_n)^2\operatorname{Im}k_n\right] \le \frac{k_0^3}{|k_n|^6}(\operatorname{Im}k_n)^3 = \theta_n''^3.$$

Hence (4.14) becomes

$$\frac{B_K \ln S_0^{-1}}{\pi} \leq k_0^3 a^3 \rho_{\nu,\nu} + \frac{\theta_0^3}{3}. \tag{A.9}$$

Combining (A.8) and (A.9) yields

$$\frac{B_K \ln S_0^{-1}}{\pi} \leq k_0^3 a^3 \rho_{\nu,\nu} + \frac{1}{3}\left(k_0 a - \frac{B_K \ln S_0^{-1}}{\pi}\right)^3,$$

with solution (4.15).

# References


[1] G. Arfken. *Mathematical Methods for Physicists.* Academic Press, Orlando, third edition, 1985.

[2] A. Bernland, A. Luger, and M. Gustafsson. Sum rules and constraints on passive systems. Technical Report LUTEDX/(TEAT-7193)/1-31/(2010), Lund University, Department of Electrical and Information Technology, P.O. Box 118, S-221 00 Lund, Sweden, 2010. `http://www.eit.lth.se`.

[3] C. F. Bohren and D. R. Huffman. *Absorption and Scattering of Light by Small Particles.* John Wiley & Sons, New York, 1983.

[4] M. R. Choi, K. J. Stanton-Maxey, J. K. Stanley, C. S. Levin, R. Bardhan, D. Akin, S. Badve, J. Sturgis, J. P. Robinson, R. Bashir, et al. A cellular Trojan horse for delivery of therapeutic nanoparticles into tumors. *Nano Letters*, **7**(12), 3759–3765, 2007.

[5] L. J. Chu. Physical limitations of omni-directional antennas. *Appl. Phys.*, **19**, 1163–1175, 1948.

[6] R. M. Fano. Theoretical limitations on the broadband matching of arbitrary impedances. *Journal of the Franklin Institute*, **249**(1,2), 57–83 and 139–154, 1950.

[7] A. A. Glazunov, M. Gustafsson, A. Molisch, and F. Tufvesson. Physical modeling of mimo antennas and channels by means of the spherical vector wave expansion. *IET Microwaves, Antennas & Propagation*, 2010. in press.

[8] M. Gustafsson, C. Sohl, and G. Kristensson. Physical limitations on antennas of arbitrary shape. *Proc. R. Soc. A*, **463**, 2589–2607, 2007.

[9] M. Gustafsson and S. Nordebo. Bandwidth, Q factor, and resonance models of antennas. *Progress in Electromagnetics Research*, **62**, 1–20, 2006.

[10] M. Gustafsson, C. Sohl, and G. Kristensson. Physical limitations on antennas of arbitrary shape. Technical Report LUTEDX/(TEAT-7153)/1–37/(2007), Lund University, Department of Electrical and Information Technology, P.O. Box 118, S-221 00 Lund, Sweden, 2007. http://www.eit.lth.se.

[11] J. E. Hansen, editor. *Spherical Near-Field Antenna Measurements.* Number 26 in IEE electromagnetic waves series. Peter Peregrinus Ltd., Stevenage, UK, 1988. ISBN: 0-86341-110-X.

[12] R. C. Hansen. *Electrically small, superdirective, and superconductive antennas.* John Wiley & Sons, New Jersey, 2006.

[13] F. W. King. *Hilbert Transforms, Volume 2.* Cambridge University Press, 2009.

[14] R. Kitamura, L. Pilon, and M. Jonasz. Optical constants of silica glass from extreme ultraviolet to far infrared at near room temperature. *Applied optics*, **46**(33), 8118–8133, 2007.

[15] R. E. Kleinman and T. B. A. Senior. Rayleigh scattering. In V. V. Varadan and V. K. Varadan, editors, *Low and high frequency asymptotics*, volume 2 of *Handbook on Acoustic, Electromagnetic and Elastic Wave Scattering*, chapter 1, pages 1–70. Elsevier Science Publishers, Amsterdam, 1986.

[16] J. Mashreghi. *Representation Theorems in Hardy Spaces.* Cambridge University Press, Cambridge, U.K., 2009.

[17] H. M. Nussenzveig. *Causality and dispersion relations.* Academic Press, London, 1972.

[18] S. J. Oldenburg, R. D. Averitt, S. L. Westcott, and N. J. Halas. Nanoengineering of optical resonances. *Chemical Physics Letters*, **288**(2-4), 243–247, 1998.

[19] E. M. Purcell. On the absorption and emission of light by interstellar grains. *J. Astrophys.*, **158**, 433–440, 1969.

[20] A. Shlivinski and E. Heyman. Time-domain near-field analysis of short-pulse antennas. I. Spherical wave (multipole) expansion. *IEEE Trans. Antennas Propagat.*, **47**(2), 271–279, February 1999.

[21] A. Shlivinski and E. Heyman. Time-domain near-field analysis of short-pulse antennas. II. Reactive energy and the antenna Q. *IEEE Trans. Antennas Propagat.*, **47**(2), 280–286, February 1999.

[22] D. Sjöberg. Variational principles for the static electric and magnetic polarizabilities of anisotropic media with perfect electric conductor inclusions. *J. Phys. A: Math. Theor.*, **42**, 335403, 2009.

[23] C. Sohl, M. Gustafsson, and G. Kristensson. Physical limitations on broadband scattering by heterogeneous obstacles. *J. Phys. A: Math. Theor.*, **40**, 11165–11182, 2007.

[24] B. Ung and Y. Sheng. Interference of surface waves in a metallic nanoslit. *Optics Express*, **15**(3), 1182–1190, 2007.

[25] M. Wohlers and E. Beltrami. Distribution theory as the basis of generalized passive-network analysis. *IEEE Transactions on Circuit Theory*, **12**(2), 164–170, 1965.

[26] D. Youla, L. Castriota, and H. Carlin. Bounded real scattering matrices and the foundations of linear passive network theory. *IRE Transactions on Circuit Theory*, **6**(1), 102–124, 1959.

[27] A. H. Zemanian. An n-port realizability theory based on the theory of distributions. *IEEE Transactions on Circuit Theory*, **10**(2), 265–274, 1963.

[28] A. H. Zemanian. *Distribution theory and transform analysis: an introduction to generalized functions, with applications.* McGraw-Hill, New York, 1965.

[29] A. H. Zemanian. *Realizability theory for continuous linear systems.* Academic Press, New York, 1972.